Nitric oxide mediates NMDA-induced persistent inhibition of protein synthesis through dephosphorylation of eukaryotic initiation factor 4E-binding protein 1 and eukaryotic initiation factor 4G proteolysis

Valérie PETEGNIEF*[1], Míriam FONT-NIEVES*, M. Elena MARTÍN[†], Matilde SALINAS[†], Anna M. PLANAS*.
*Departamento de Isquemia Cerebral y Neurodegeneración,
Instituto de Investigaciones Biomédicas de Barcelona, CSIC-IDIBAPS,
Rosselló 161, Barcelona 08036, Spain
Phone: +34 93 363 83 00 (ext. 359)
Fax: +34 93 363 83 01
[†] Departamento de Bioquímica-Investigación,
Hospital Ramón y Cajal, Madrid 28034, Spain
[1] To whom correspondence should be addressed (e-mail vpefat@iibb.csic.es)

Short title: Dephosphorylation of 4E-BP1 and proteolysis of eIF4G after NMDA lesion

Key words: 4E-BP1, eIF4G, calpain, excitotoxicity, ischemia, NO.

Abbreviations used: eIF2α, eukaryotic initiation factor 2α; eIF4E, eukaryotic initiation factor 4E; eIF4G, eukaryotic initiation factor 4G; 4E-BP1: eukaryotic initiation factor 4E-binding protein 1, mTOR, mammalian target of rapamycin; NOSI: NOS inhibitors (NAME+NPLA); DEA/NO, Diethylamine/Nitric oxide sodium complex.

Abstract

Cerebral ischemia causes long-lasting protein synthesis inhibition that is believed to contribute to brain damage. Energy depletion promotes translation inhibition during ischemia and the phosphorylation of eukaryotic initiation factor 2α (eIF2α) is involved in the translation inhibition induced by early ischemic reperfusion. However, the molecular mechanisms underlying prolonged translation downregulation remain elusive. NMDA excitotoxicity is also involved in ischemic damage, as exposure to NMDA impairs translation and promotes the synthesis of nitric oxide (NO), which can also inhibit translation. Here we investigated whether NO was involved in NMDA-induced protein synthesis inhibition in neurons and studied the underlying molecular mechanisms. NMDA and the NO-donor DEA/NO both inhibited protein synthesis and this effect persisted after a 30-min-exposure. Treatments with NMDA or NO promoted calpain-dependent eIF4G cleavage and 4E-BP1 dephosphorylation and also abolished the formation of eIF4E/eIF4G complexes, however they did not induce eIF2α phosphorylation. Although NO synthase (NOS) inhibitors did not prevent protein synthesis inhibition during 30-min NMDA exposure, they did abrogate the persistent inhibition of translation observed after NMDA removal. NOS inhibitors also prevented NMDA-induced eIF4G degradation, 4E-BP1 dephosphorylation, eIF4E-eIF4G binding reduction and cell death. Although the calpain inhibitor calpeptin blocked NMDA-induced eIF4G degradation, it did not prevent 4E-BP1 dephosphorylation, which precludes eIF4E availability, and thus translation inhibition was maintained. This study suggests that eIF4G integrity and hyperphosphorylated 4E-BP1 are needed to ensure appropriate translation in neurons. In conclusion, our data show that NO mediates NMDA-induced persistent translation inhibition and suggest that deficient eIF4F activity contributes to this process.

INTRODUCTION

Brain ischemia induces early and deep inhibition of protein synthesis that is persistent in vulnerable neurons such as CA1 hippocampal and striatal neurons [1-3]. In this regard, long-lasting inhibition of protein synthesis is one of the alterations that best correlates with neuronal injury after ischemia. Indeed, translation recovery is associated with survival, whereas neurons unable to overcome protein synthesis blockade are destined to die [4]. Translation is mainly inhibited via regulation of the initiation and elongation steps, by impairing the activity of certain eukaryotic initiation or elongation factors (eIFs or eEFs). Modulation of the phosphorylation status and/or degradation of these proteins account for their inactivation. For instance, changes in the phosphorylation status of eIF2α, 4E-BP1 or eEF2 are known to modulate the rate of protein synthesis [5]. Phosphorylation of eIF2α by the double-stranded RNA-activated protein kinase-like endoplasmic reticulum (ER) kinase (PERK) is sufficient to abrogate protein synthesis soon after reperfusion following an ischemic episode [6-9]. In addition, a number of other factors are affected. For instance, depletion of ATP activates eEF2 kinase through AMP kinase in cortical neurons and slows elongation [10]. Furthermore, global cerebral ischemia leads to eIF4G and eIF4E breakdown [11-13]. Production of NO bursts after ischemia and NO is involved in inflammation, cerebral damage [14] and protein synthesis reduction through eIF2α phosphorylation [15-17].

Likewise, excitotoxicity is one of the main promoters of neuronal loss after an ischemic episode, and is also known to inhibit protein synthesis [18-21]; however the underlying mechanisms are not fully elucidated. The rise in intracellular calcium induced by glutamate activates eEF2 kinase, which in turn phosphorylates eEF2 and results in the transient blockade

of elongation [18]. The increase in cytosolic calcium concentration following NMDA activates the cysteine protease calpain [22]. eIF4G, the scaffolding protein that enables the assembly of eIF4E and eIF4A with the mRNA and the ribosomal 40S subunit is a substrate of calpain [13], and is thus a possible target of NMDA. However, most studies of eIF4G cleavage have reported that eIF4G is the target of caspase-3 in apoptotic conditions (reviewed in [23]). Caspase-3 cuts eIF4GI at two sites to generate three fragments, as referred to as: **F**ragments of **A**poptotic cleavage of eIF4**G** (FAG): N-FAG, M-FAG and C-FAG, corresponding to the N-, middle- and C-terminal parts of the protein, respectively (reviewed in [23]). M-FAG$_{533\text{-}1176}$ is the only fragment that remains able to promote some cap-dependent translation. Therefore, proteolysis of eIF4G is presumably associated with the switch from cap-dependent to cap-independent translation and favours, for example, the translation of specific internal ribosome entry site (IRES)-containing mRNAs [23]. Unlike with FAG, the role of eIF4G fragments resulting from calpain activity has not been explored.

eIF4E binding protein 1 (4E-BP1) is another key regulator in protein synthesis because it associates to eIF4E [24]. In cell cultures, insulin, amino acids and rapamycin modulate the phosphorylation status of 4E-BP1 through mammalian target of rapamycin (mTOR) signalling [25,26]. In the hypophosphorylated form, 4E-BP1 competes with the binding site of eIF4G and sequesters eIF4E, whereas the hyperphosphorylated γ form dissociates from eIF4E, enabling it to engage with other components of the eIF4F complex [24,27-31]. Therefore, proteolysis of eIF4G together with dephosphorylation of 4E-BP1 precludes the formation of eIF4F complexes [32] that may reduce the cap-mRNA translation.

There is compelling evidence of crosstalk between NO and NMDA. In pure neuron cultures, uncoupling between the NMDA receptor and nNOS signaling pathways [33] and pharmacological inhibition of nNOS [34] strongly prevent neuronal death after an excitotoxic challenge. Reciprocally, production of NO by iNOS in activated glia leads to neuronal death, which is prevented by MK-801, a NMDA receptor antagonist [35-37], thus suggesting that NO leads to glutamate release [38] in a positive feed-back loop. Furthermore, NO challenge triggers excitotoxicity in cerebellar neurons [39]. The mechanisms responsible for NO toxicity are not completely elucidated but energy depletion is likely involved. NO induces a fast depolarisation of the mitochondria, which leads to reduced ATP production [40]. In addition, NO exposure triggers the activation of PARP that leads to ATP consumption and may therefore account for energy depletion [41].

Here we addressed the molecular mechanisms underlying NMDA-mediated long-term inhibition of protein synthesis in neuronal cultures, and considered whether NO is involved in this process.

MATERIALS AND METHODS

Materials

All products for culture, except MEM, were purchased from Invitrogen (Paisley, Scotland, UK). ATP bioluminescent assay kit, somatic cell ATP releasing agent, chemicals and reagents were obtained from Sigma-Aldrich (Alcobendas, Spain), unless otherwise stated. Diethylamine/Nitric oxide sodium complex (DEA/NO) and Nω-propyl-L-arginine were purchased from Tocris (Avonmouth, UK). The calpain inhibitors calpeptin and MDL28170, as well as rapamycin were from Calbiochem (LaJolla, CA, USA). The non-specific nitric oxide synthase (NOS) inhibitor Nω-nitro-L-arginine methyl ester (L-NAME) and the neuronal specific NOS (nNOS) inhibitor Nω-propyl-L-arginine (NPLA) were purchased from Sigma-Aldrich. The mouse antibodies against eIF4E and STAT3 were from BD Transduction Laboratories (Heidelberg, Germany). The goat antibodies against eIF4G (N-20) and anti-

eIF2α were purchased from Santa Cruz Biotechnology (Heidelberg, Germany). Rabbit anti-phospho-eIF2α (Ser^{51}) was from Epitomics (Burlingame, CA, USA) and mouse anti-spectrin was from Chemicon (Temecula, CA, USA). Anti-4E-BP1 antibody was obtained from Cell Signaling Technology (Beverly, MA, USA). Anti-mouse, anti-goat and anti-rabbit HRP-conjugated antibodies were from Amersham (Buckinghamshire, England). Complete protease inhibitor cocktail and the antibody against β-tubulin were from Boehringer Mannheim (Germany). L-[4,5-^{3}H]leucine (S.A. = 73 Ci/mmol) and 7-methyl GTP-Sepharose were purchased from Amersham (Buckinghamshire, England).

Cell cultures and treatments

Mixed primary cortical cultures of neurons and glia were prepared from 18-day-old Sprague-Dawley rat embryos (Charles River, France), as previously described [20]. Animals were anaesthetized and killed by cervical dislocation. All procedures were approved by the Ethical Committee for Animal Use (CEEA) at the University of Barcelona. Neuron-enriched cultures were prepared as mixed cultures, but ARA-C was added on day in vitro 4 and then in the subsequent partial medium changes on days in vitro 7 and 10 to limit glial proliferation. Cells were seeded on 24-well plates at a density of 3680 cells/mm^2. For the ATP content measurement, cells were seeded on 6-well plates. All experiments were performed on day in vitro 11-13 cultures.

DEA/NO was prepared as a 20 mM stock in NaOH pH10 to avoid NO release and stored at -20ºC for further use. A 2 mM DEA/NO solution in NaOH pH10 was prepared extemporaneously and added to the culture medium in order to achieve a final concentration of 4-40 µM. Cells were exposed for 30 min to DEA/NO and medium was thereafter replaced with MEM supplemented with B27 and gentamycin. Excitotoxic lesion was performed by treating cultures for 30 min with 35 µM NMDA. NOS inhibitors (L-NAME + NPLA) were added simultaneously to NMDA and also after medium change. Calpain inhibitors were added at 30 µM, unless otherwise stated, 1 h before NMDA or DEA/NO and also after medium change. Thapsigargin at 1 or 10 µM was added for 30 min and rapamycin at 1 or 2 µM for 3 h with no previous medium change. Calpeptin, MDL28170, thapsigargin and rapamycin were dissolved in DMSO.

Measurement of LDH activity

Cell death was estimated 24 h after the lesion by measuring the activity of lactate dehydrogenase (LDH) released in the medium as previously described [20]. Briefly, the decrease in 0.75 mM NADH absorbance at 340 nm was followed in a phosphate buffer (50 mM, pH 7.4) in the presence of 4.2 mM pyruvic acid as substrate. The kinetic assay of NADH consumption was monitored for 4 min and the slope values of decreased absorbance at 340 nm (negative values) were converted to positive values and expressed in arbitrary units (AU).

Propidium iodide nuclear staining

Cells were treated for 30 min with 35 µM NMDA and then fixed and stained with propidium iodide (PI) 24 h later as previously described [20]. PI-positive nuclei were counted in three fields per well and the sum of the three, corresponding to a total area of 0.4416 mm^2 was calculated. The result was expressed as PI positive cells/mm^2.

Incorporation of [^{3}H]leucine into proteins

Culture medium was withdrawn and cells were incubated in 300 µl of MEM/B27 containing 396 µM of unlabeled leucine and 4 µCi/ml [^{3}H]leucine for 30 min at 37ºC. NMDA or DEA/NO were added immediately after the [^{3}H]leucine to evaluate their effect on protein synthesis at 30 min (0.5 h in figures). To assess protein synthesis 2 h after transient exposure

to NMDA or DEA/NO, cells were incubated with NMDA or DEA/NO for 30 min, medium was changed to MEM/B27 and, 90 min later, cells were incubated with [^{3}H]leucine for 30 min as described above. Medium was removed, proteins were precipitated with trichloroacetic acid and lysates were processed as previously described [20] for the determination of [^{3}H]leucine incorporated into proteins. Results were expressed as dpm in the TCA fraction/mg protein/min.

Measurement of ATP levels

After drug treatments, cells were washed with cold PBS and collected in a 5 mM EDTA, 0.1 M Na_2HPO_4, pH 7.5 buffer. After a 5 min spin at 590 X g at 4ºC, pellets were resuspended in 200 µl of the same buffer, sonicated and centrifuged again for 15 min at 10 000 X g at 4ºC. ATP content was determined in the fresh supernatants using an ATP bioluminescent assay kit and following manufacturer's instructions. Samples were run together with a 0.05-8 µM ATP standard curve and luminescence was monitored in an Orion microplate luminometer (Berthold detection system). Relative light units (RLU) were converted to pmols of ATP and results were expressed as nmol ATP/mg protein.

Western blot

Neuron-enriched cultures were treated with NMDA, NMDA+NOS inhibitors, or DEA/NO for 30 min. Ninety minutes later, cultures were washed with cold 10 mM phosphate-buffered saline (PBS) and harvested in radio-immunoprecipitation (RIPA) lysis buffer (10 mM PBS, 1% Igepal AC-630, 0.5% sodium deoxycholate, 0.1% sodium dodecyl sulphate) supplemented with a protease inhibitor cocktail (Complete) and 1 mM sodium orthovanadate. Protein content was determined by the Bradford assay (Bio-Rad Laboratories, München, Germany). Thirty µg of proteins was separated by electrophoresis on 7%, 12% or 17% polyacrylamide gels (for spectrin-eIF4G, eIF2α and 4E-BP1, respectively) in denaturing conditions and transferred to 0.2 µm polyvinylidene difluoride Immun-Blot membranes (Bio-Rad Laboratories, Hercules, CA, USA). Membranes were incubated overnight at 4ºC with the following primary antibodies: goat anti-eIF4G diluted 1:500, goat anti-eIF2α, rabbit anti-phospho-eIF2α (Ser^{51}), rabbit anti-4E-BP1 diluted 1:2000, mouse anti-spectrin diluted 1:4000, mouse anti-STAT3 and mouse anti-eIF4E diluted 1:1000. After two washes in Tris buffer containing Tween-20 (T-TBS), membranes were then incubated for 1 h at room temperature with either anti-rabbit, anti-mouse or anti-goat horseradish peroxidase-conjugated antibody. The reaction was visualized using a chemiluminescence detection system based on the luminol reaction. Autoradiograms were scanned with a GS-800 Densitometer scanner (Bio-Rad) and band density was quantified with the Quantity One image analysis software (Bio-Rad). Molecular weight markers are indicated in kDa on the left side of some of the blots shown in the Figures. For the analysis of eIF2α phosphorylation the phosphorylated/total protein ratio was calculated for each sample. Since the molecular weights of spectrin and eIF4G are 240 and 220 kDa, respectively, we decided to use the 90 kDa protein STAT3 of higher MW than tubulin, to check for equal loading, since none of the treatments affected STAT3 expression (not shown). The densities of the 150-145 kDa bands corresponding to cleaved spectrin were quantified together. The spectrin/STAT3 and eIF4G/STAT3 ratios were calculated for each sample. Data from all quantifications are expressed as a percentage of controls. In the case of 4E-BP1, the proportion of each phosphorylated form (α, β and γ) was calculated as a percentage of total 4E-BP1 as in [32].

Determination of the formation of eIF4E/eIF4G and eIF4E/eIF4E-B1 complexes

After the different treatments, cells were washed with buffer A containing 20 mM Tris-HCl, pH 7.6, 1 mM dithiothreitol, 1 mM EDTA, 1 mM PMSF, 1 mM benzamidine, 120 mM KCl,

10 μg/ml leupeptin, 1 μg/ml pepstatin A, 10 μg/ml antipain, 50 mM sodium fluoride, 10 mM glycerophosphate and 10 mM sodium molybdate; they were then lysed with buffer A containing 0.5% Igepal AC-630 and 0.1% triton X-100. Cell extracts were spun at 12000 X g for 10 min at 4ºC and the supernatants were collected and frozen at -80ºC for further use. Two hundred μg of proteins was incubated with 7-methylguanosine triphosphate (m^7GTP)-Sepharose for 45 min at 4ºC in buffer A containing 0.1 mM GTP. Proteins were eluted from m^7GTP-Sepharose with SDS loading buffer and subjected to 7.5%-17% SDS-PAGE and Western blot. Membranes were incubated separately with antibodies against eIF4G, eIF4E and 4E-BP1.

Statistical analysis

Results are expressed as mean ± SEM and the number of replicates (n) is indicated in the legend of each figure. Unless indicated, one-way analysis of variance (ANOVA) with the Bonferroni *post-hoc* test was performed to evaluate significant differences between groups. Kruskal-Wallis analysis followed by Dunn's test for multiple comparisons was used to compare groups with non-homogenous variance. One symbol indicates $P<0.05$, two $P<0.01$ and three $P<0.001$.

RESULTS

NOS inhibitors protected against NMDA toxicity in mixed and neuron-enriched cultures.

One of our objectives was to determine whether NO participates in NMDA-induced inhibition of protein synthesis in our primary cultures. First, we confirmed that NMDA toxicity was dependent on NO. When testing the effect of several NOS inhibitors we found that the combination of the non-specific NOS inhibitor L-NAME with the specific nNOS inhibitor NPLA at 2 mM and 100 μM, respectively provided almost complete protection against transient (30 min) exposure to 35 μM NMDA in mixed neuron/glia and neuron-enriched cultures, as assessed by lactate dehydrogenase activity and propidium iodide staining assays (Figs. 1A and 1B). Further experiments were therefore performed with the NAME+NPLA combination of NOS inhibitors (referred to as NOS inhibitors in the text). Treatment with the above concentrations of NOS inhibitors did not affect neuronal viability (Fig. 1A). To check for direct NO toxicity, i.e. not induced by NMDA, we performed a dose-response study with DEA/NO, an NO-donor. DEA/NO was applied for 30 min and toxicity was assessed at 24 h. At 40 μM DEA/NO induced similar toxicity to treatment with 35 μM NMDA (Fig. 1C) and this concentration of DEA/NO was therefore selected to perform further experiments.

NMDA and NO induced protein synthesis failure

We have previously demonstrated that NMDA decreases the protein synthesis rate after 1 h exposure [20]. Here we explored whether transient exposure to NMDA caused long-lasting inhibition of protein synthesis. A time-course study showed that NMDA inhibited by 52 and 43% the incorporation of [^{3}H]leucine into proteins after 30-min exposure in mixed (Fig. 2A) and neuron-enriched cultures (Fig. 2B), respectively. After removal of NMDA, protein synthesis partially recovered but remained significantly lower than in controls 2 h later (i.e. 90 min after NMDA removal) in both mixed (Fig. 2A) and neuron-enriched cultures (Fig. 2B). NOS inhibitors were ineffective at 30 min (during NMDA exposure) but did promote complete recovery of protein synthesis at 2 h. Treatment with NOS inhibitors alone had no effect on protein synthesis (Fig. 2B). DEA/NO also led to a slight reduction of protein synthesis (less than 20%) at the end of a 30-min exposure and the effect was more

pronounced 2 h later (33% decrease) in neuron-enriched cultures (Fig. 2C). Altogether these data suggest that NO impairs translation and contributes to the late phase of protein synthesis inhibition induced by NMDA.

NMDA and NO induced a moderate decrease in ATP content and did not regulate the phosphorylation of eIF2α

ATP depletion can induce endoplasmic reticulum stress, which leads to phosphorylation of eIF2α and subsequent inhibition of protein synthesis [15,42]. Here we evaluated ATP content after the treatments to determine whether ATP depletion was involved in the observed inhibition of protein synthesis. NMDA caused a 26% reduction of ATP levels at the end of the 30-min exposure, and this effect was maintained 2 h later (Fig. 3A). Although DEA/NO reduced ATP content to 53% after 30-min exposure, this effect was not significantly different from controls 2 h later (Fig. 3B), thus indicating that in contrast to NMDA the action of NO on ATP is not long-lasting. NOS inhibitors did not prevent the ATP decrease 2 h after NMDA exposure (Fig. 3C), and this illustrates that NO was not involved in the persistent ATP reduction after NMDA. Our data suggest that the late protein synthesis inhibition caused by NMDA is not mediated by the corresponding ATP reduction.

Phosphorylated eIF2α binds to the GDP/GTP exchanger eIF2B and inhibits its function ([reviewed in [30]). The inability to restore the binding of GTP to eIF2 prevents the formation of new eIF2·GTP·Met-tRNAi ternary complexes and consequently protein synthesis is inhibited. NMDA and NO did not induce eIF2α phosphorylation on Ser^{51} (Figs. 3D and 3E), indicating that eIF2 activity was not inhibited. In order to determine whether our cultures might show increased phosphorylation of eIF2α, neurons were treated for 30 min with thapsigargin. This endoplasmic reticulum stress inducer is known to cause eIF2α phosphorylation through PERK activation. Figure 3F shows that thapsigargin triggers eIF2α phosphorylation when compared to control cells.

NMDA and NO led to calpain activation and eIF4G proteolysis

NMDA is known to induce cytosolic calcium increase [10,20] during the period of exposure. As expected, NMDA activated calpain, a calcium-dependent cysteine protease, which was assessed by the proteolysis of α-spectrin (Figs. 4A and 4C). The 240 kDa full-length protein is processed into 150 and 145 kDa fragments by calpain and to 150 kDa and 120 kDa fragments by caspase-3 [43]. NMDA generated the formation of the 145-150 kDa fragments only (Fig. 4A), this being indicative of calpain-dependent hydrolysis. Furthermore, eIF4G was cleaved 2 h after NMDA exposure (39% decrease, $P<0.05$; Figs. 4A and 4C). Proteolysis of both spectrin and eIF4G was completely blocked in the presence of NOS inhibitors (Figs. 4A and 4C), thus indicating an NO-dependent mechanism. In agreement with a previous report [39], NO dramatically stimulated calpain and reduced eIF4G levels by 52% (Figs. 4B and 4D). Several calpain inhibitors (not shown) were then used to determine the contribution of calpain to eIF4G processing, and we found that two of them, calpeptin and MDL28170, completely inhibited calpain activation and blocked the eIF4G degradation induced by NMDA (Figs. 5A and 5C) and DEA/NO (Figs. 5B and 5D). Therefore, eIF4G degradation was totally dependent on calpain activation.

NMDA and DEA/NO induced the dephosphorylation of 4E-BP1 and abrogated the formation of eIF4F complexes

The formation of eIF4F complexes plays a key role in the regulation of translation initiation. Since eIF4E is a component of the eIF4F complex and it is a rate-limiting translation factor for cap-mRNA, we measured its level of expression, observing that none of the treatments altered its cell content (Fig. 6A).

The phosphorylation status of 4E-BP1 also governs the formation of eIF4F complexes. 4E-BP1 resolves into three electrophoretic forms γ, β and α of increasing migration velocity. Only the hyperphosphorylated γ form of 4E-BP1 does not bind eIF4E [31] and therefore it increases the availability of eIF4E to interact with eIF4G. We studied the phosphorylation of 4E-BP1 and performed a semi-quantitative analysis of the proportion of γ, β and α forms with respect to total 4E-BP1 (Fig. 6B and Table 1). NMDA was observed to promote a shift from the γ form to the α form (Table 1), an effect that was abrogated by NOS inhibitors (Fig. 6B and Table 1). Furthermore, DEA/NO induced the dephosphorylation of 4E-BP1, illustrated by a decrease in the γ form and an increase in the α form, which is the band of lowest mobility (Fig. 6B and Table 1). In contrast, none of the treatments affected the β form.
Since eIF4G and 4E-BP1 compete for the same binding site in eIF4E, we evaluated the proteins bound to eIF4E after its purification by m^7GTP-sepharose affinity chromatography. DEA/NO and NMDA almost completely abolished the interaction between eIF4G and eIF4E, and the NMDA effect was prevented by NOS inhibitors (Fig. 6C).
We also studied whether calpain inhibitors influenced the phosphorylation status of 4E-BP1. Calpeptin and MDL28170 did not reverse the dephosphorylation of 4E-BP1 induced by NMDA and DEA/NO, respectively (Fig. 6B and Table 1). Moreover, calpeptin decreased the γ form and enhanced the formation of the α form compared to NMDA alone (Fig. 6B and Table 1). When the protein synthesis rate was measured, we observed that none of the calpain inhibitors prevented the blockade of protein synthesis induced by NMDA or DEA/NO (Fig. 6D), thus suggesting that the prevention of eIF4G cleavage alone is not sufficient to abrogate the inhibition of protein synthesis. In contrast, NOS inhibitors that blocked eIF4G processing and dephosphorylation of 4E-BP1 did promote the complete recovery of translation (Figs. 2B, 4C and 6B). In addition, we observed that none of the calpain inhibitors rescued neurons from death (Fig. 6E), suggesting that survival is compromised when the normal rate of protein synthesis is not achieved.

Rapamycin reduced the formation of eIF4F complexes and inhibited protein synthesis in a similar way to NMDA

In order to determine whether hypophosphorylation of 4E-BP1 was by itself sufficient to reduce the formation of eIF4F complexes in the absence of eIF4G degradation, we incubated neurons with rapamycin, an inhibitor of the 4E-BP1 kinase mTOR (reviewed in [30]). Three hours after addition of rapamycin we observed a dephosphorylation of 4E-BP1 but no loss of eIF4G (Fig. 7A). When we looked at the amount of eIF4G bound to eIF4E after m^7GTP-sepharose affinity chromatography, we found that rapamycin induced a dose-dependent inhibition of eIF4G binding to eIF4E (Fig. 7B) that correlated with a decrease in protein synthesis (Fig. 7C) of similar proportions to that achieved with NMDA (Fig. 6D).

DISCUSSION

The present study investigated the mechanisms underlying excitotoxicity-mediated translation repression. In particular, we explored the contribution of eIF4G proteolysis and 4E-BP1 dephosphorylation to NMDA- and DEA/NO-induced protein synthesis inhibition. To our knowledge, this is the first study to report molecular changes in translation factors that might be involved in the long-lasting inhibition of protein synthesis after transient exposure to NMDA. We showed that neurons can withstand a transient blockade of translation with limited neuronal loss, and also provided evidence that protein synthesis recovery closely correlates with neuronal survival, as is observed in animal models of stroke [1]. Indeed, the inactivation of NOS enabled full recovery of global protein synthesis, along with an almost complete rescue from NMDA-induced neurotoxicity; this latter finding has been previously

reported by other groups [44,45]. Interestingly, NOS inhibitors were able to prevent the delayed but not the initial inhibition of protein synthesis following NMDA exposure. Similarly, ischemic preconditioning suppresses persistent but not acute inhibition of translation (reviewed in [46]).

NOS inhibitors did not impede NMDA-induced ATP reduction, despite the fact that they promoted a complete recovery of protein synthesis. Therefore, the moderate decrease in ATP after NMDA and DEA/NO treatments is unlikely to be the cause of protein synthesis inhibition. This result is in agreement with previously published data showing that severe protein synthesis inhibition precedes ATP reduction after treatment with an NO-donor [17]. Furthermore, suppression of protein synthesis occurs in the penumbra where ATP levels are maintained in transient focal ischemia [3]. Interestingly, our data are in accordance with studies suggesting that transient inhibition of protein synthesis is not lethal, whereas the persistent phase of translation suppression is related to neurodegeneration [18,46-48].

Release of calcium from ER stores through blockade of Ca^{2+}/ATPase with thapsigargin [17] was shown to induce protein synthesis alterations due to phosphorylation of eIF2α. Glutamate also mobilizes Ca^{2+} from ER reservoirs but depresses protein synthesis in an eIF2α phosphorylation-independent manner [19], in agreement with our data. We did not detect phosphorylation of eIF2α after exposure to DEA/NO, a fast NO-releasing complex, in contrast to previous observations in neuroepithelial cells [16]. S-nitroso–N-acetylpenicillamine (SNAP), a slow NO-releasing agent, has been shown to mobilize thapsigargin-sensitive calcium ER stores in neurons [17] and to phosphorylate eIF2α similarly to thapsigargin in neuroblastoma [15]. The shorter exposure time, faster NO release and lower concentration of NO-donor used in our study may explain the discrepancies with those studies. Therefore, under our experimental conditions DEA/NO inhibited translation by a mechanism that was independent of eIF2α phosphorylation, at least in the late phase. Our data suggest that NO does not contribute to the initial inhibition of protein synthesis by NMDA, but rather takes part in delayed translation deterioration.

Calpain activation and subsequent proteolysis of its substrates is known to occur after excitotoxicity in neurons [22,39,43]. While some reports show an attenuation of NMDA toxicity with pharmacological inhibitors of calpain [22], others have found no protection [43], as we did in the present study. Nevertheless, we found that calpain was responsible for eIF4G breakdown after exposure to NMDA or DEA/NO, in accordance with previous observations in the ischemic brain [13]. Proteolysis of several translation factors has been reported, mainly in apoptotic conditions. Research has shown that eIF2α and 4E-BP1 are the substrate for caspase-3 (reviewed in [23]), while eIF4E and 4E-BP1 are the substrate for calpain *in vitro* [12,49]. However, to the best of our knowledge there is no evidence that eIF4E and 4E-BP1 are cleaved by calpain *in vivo* [12,49]. Here, we did not observe any degradation of eIF2α, eIF4E or 4E-BP1, suggesting that calpain specifically processed eIF4G in our settings. The eIF4G fragment generated by calpain cleavage does not bind to eIF4E, thus precluding the formation of eIF4F complexes, as shown in both the present study and a model of global cerebral ischemia [32]. Therefore, it is likely that the strong proteolysis of eIF4G contributed to impaired translation in our experimental conditions.

The binding of 4E-BP1 to eIF4E also compromises the association of eIF4F components [24]. We observed that NMDA and DEA/NO insults led to the dephosphorylation of 4E-BP1, which is expected to facilitate its binding to eIF4E. A similar process has been described after global ischemia and was shown to cause a deficit in eIF4E/eIF4G complexes and, therefore, to contribute to translation inhibition [32]. NOS inhibitors enabled the complete recovery of protein synthesis by preventing eIF4G proteolysis and by precluding the dephosphorylation of 4E-BP1. The lack of protein synthesis recovery in the presence of a normal amount of eIF4G (in the presence of calpain inhibitors) suggests that

the hypophosphorylation of 4E-BP1 is sufficient to reduce the protein synthesis rate. This result is supported by the data obtained with rapamycin. Rapamycin that dephosphorylated 4E-BP1 but maintained eIF4G integrity reduced the rate of protein synthesis. The rapamycin-induced inhibition of translation correlated with the reduced formation of eIF4E/eIF4G complexes. eIF4E is crucial for cap-dependent translation initiation and is a mandatory element of the eIF4F complex since it functions as the cap-binding protein. Reduced availability of eIF4E resulting from protease-mediated degradation or trapping by 4E-BP1 would severely compromise cap-mRNA translation. Therefore, eIF4E is a rate-limiting factor and its sequestration by 4E-BP1 might slowdown the process of translation. The lower amount of full-length eIF4G may worsen the process by decreasing the probability of eIF4E-eIF4G binding. Our data suggest that preventing eIF4G degradation and 4E-BP1 dephosphorylation are necessary to unlock translation repression. The maintenance of eIF4G levels while 4E-BP1 is hypophosphorylated is not sufficient to prevent protein synthesis inhibition. Our results are in agreement with research showing that ischemic tolerance, which promotes translation recovery, tends to prevent eIF4G processing and to favour the phosphorylation of 4E-BP1 [47,50].

Since eIF4G and eIF4E play a key role in the translation of cap-mRNAs, we propose that limited availability of both proteins accounts for long-lasting translation failure (summarized in Figure 8) and contributes to neuronal loss after NMDA and NO challenges. Further studies are required to unravel the mechanisms controlling 4E-BP1 dephosphorylation.

Acknowledgements:
The authors would like to thank Araceli Salinas and Elisabet Gomez for their excellent technical assistance and the Language Advice Service from the University of Barcelona for revising the English. VP is a recipient of a Ramon y Cajal grant and MFN a recipient of a FPI grant from the Spanish Ministry of Education and Science (MEC). This study was supported by grants FIS05/0271 from the Spanish Ministry of Health and SAF2005-05793-C01 from the Ministry of Education and Science.

REFERENCES

1 Hossmann, K.A. (1993) Disturbances of cerebral protein synthesis and ischemic cell death. Prog. Brain Res. **96** 161-177

2 Dienel, G.A., Pulsinelli, W.A. and Duffy, T.E. (1980) Regional protein synthesis in rat brain following acute hemispheric ischemia. J. Neurochem. **35** 1216-1226

3 Hata, R., Maeda, K., Hermann., D and Hossmann, K.A. (2000) Evolution of brain infarction after transient cerebral ischemia in mice. J. Cereb. Blood Flow Metab. **20** 937-946

4 Hermann, D.M., Kilic E., Hata R., Mies, G., and Hossmann, K.A. (2001) Relationship between metabolic dysfunctions, gene responses and delayed cell death after focal cerebral ischemia in mice. Neuroscience **104** 947-955

5 Rhoads. RE (1999) Signal transduction pathways that regulate eukaryotic protein synthesis J. Biol. Chem. **274** 30337-30340

6 Burda, J., Martin, M.E., Garcia, A., Alcazar, A., Fando, J.L. and Salinas, M. (1994) Phosphorylation of the α subunit of initiation factor 2 correlates with the inhibition of translation following transient cerebral ischaemia in the rat. Biochem. J. **302** 335-338

7 DeGracia, D.J., Adamczyk, S., Folbe, A.J., Konkoly, L.L., Pittman, J.E., Neumar, R.W., Sullivan, J.M., Scheuner, D., Kaufman, R.J., White, B.C. and Krause, G.S. (1999) Eukaryotic initiation factor 2α kinase and phosphatase activity during postischemic brain reperfusion. Exp. Neurol. **155** 221-227

8 Kumar, R., Azam, S., Sullivan, J.M. , Owen, C.R., Cavener, D.R., Zhang, P., Ron, D., Harding, H.P., Chen, J.J., Han, A.,White, B.C., Krause, G.S. and DeGracia, D.J. (2001) Brain ischemia and reperfusion activates the eukaryotic initiation factor 2α kinase, PERK J. Neurochem. **77** 1418-1421

9 Paschen, W., Aufenberg, C., Hotop, S. and Mengesdorf T. (2003) Transient cerebral ischemia activates processing of xbp1 messenger RNA indicative of endoplasmic reticulum stress. J. Cereb. Blood Flow Metab. **23** 449-461

10 Maus, M., Torrens, Y., Gauchy, C., Bretin, S., Nairn, A.C., Glowinski, J. and Premont, J. (2006) 2-Deoxyglucose and NMDA inhibit protein synthesis in neurons and regulate phosphorylation of elongation factor-2 by distinct mechanisms. J. Neurochem. **96** 815-824

11 DeGracia, D.J., Neumar, R.W., White, B.C. and Krause, G.S. (1996) Global brain ischemia and reperfusion: modifications in eukaryotic initiations factors associated with inhibition of translation initiation. J. Neurochem. **67** 2005-2012

12 Neumar, RW, DeGracia, D.J., White, B.C., McDermott, P.J., Evans, D.R. and Krause, G.S. (1995) Eukaryotic initiation factor 4E degradation during brain ischemia. J. Neurochem. **65** 1391-1394

13 Neumar, R.W., DeGracia, D.J., Konkoly, L.L., Khoury, J.I., White, B.C. and Krause, G.S. (1998) Calpain mediates eukaryotic initiation factor 4G degradation during global brain ischemia. J. Cereb. Blood Flow Metab. **18**, 876-881

14 Warner, D.S., Sheng, H. and Batinic-Haberle, I. (2004) Oxidants, antioxidants and the ischemic brain. J. Exp. Biol. **207**, 3221

15 DeGracia, D.J. and Montie, H.L. (2004) Cerebral ischemia and the unfolded protein response. J. Neurochem. **91**, 1-8

16 Uma, S., Yun, B.G. and Matt, R.L. (2001) The heme-regulated eukaryotic initiation factor 2α kinase. J. Biol. Chem. **276**, 14875-14883

17 Doutheil, J., Althausen, S., Treiman, M. and Paschen W (2000) Effect of nitric oxide on endoplasmic reticulum calcium homeostasis, protein synthesis and energy metabolism. Cell Calcium **27**, 107-115

18 Marin, P., Nastiuk, K.L., Daniel, N., Girault, J.A., Czernik, A.J., Glowinsky, J., Nairn, A.C. and Premont J. (1997) Glutamate-dependent phosphorylation of elongation factor-2 and inhibition of protein synthesis in neurons. J. Neurosci. **17**, 3445-3454

19 Gauchy, C., Narin, A.C., Glowinski, J. and Premont J. (2002) N-methyl-D-aspartate receptor activation inhibits protein synthesis in cortical neurons independently of its ionic permeability properties. Neuroscience **114**, 859-867

20 Petegnief, V., Friguls, B., Sanfeliu, C., Suñol C. and Planas, A.M. (2003) Transforming growth factor-α attenuates NMDA toxicity in cortical cultures by preventing protein synthesis inhibition through an Erk1/2-dependent mechanism. J. Biol. Chem. **278**, 29552-29559

21 Cossenza, M., Cadihle, D.V., Coutinho, R.N., Coutinho, R.N. and Paes-de-Carvalho, R. (2006) Inhibition of protein synthesis by activation of NMDA receptors in cultured retinal neurons: a new mechanism for the regulation of nitric oxide production. J. Neurochem. **97**, 1481-1493.

22 Tremblay, R., Chakravarthy, B., Hewitt, K., Tauskela, J., Morley, P., Atkinson, T. and Durkin, J.P. (2000) Transient NMDA receptor inactivation provides long-term protection to cultured cortical neurons from a variety of death signals. J. Neurosci. **20**, 7183-7192

23 Morley, S.J., Coldwell, M.J., and Clemens, M.J. (2005) Initiation factor modifications in the preapototic phase. Cell Death Differ. **12**, 571-584.

24 Haghighat, A., Mader, S., Pause, A. and Sonenberg, N. (1995) Repression of cap-dependent translation by 4E-binding protein 1: competition with p220 for binding to eukaryotic initiation factor-4E. EMBO J. **14**, 5701-5709

25 Mothe-Satney, I., Brunn, G.J., McMahon, L.P., Capaldo, C.T., Abraham, R.T. and Lawrence, J.C. Jr. (2000) Mammalian target of rapamycin-dependent phosphorylation of PHAS-I in four (S/T)P sites detected by phosphor-specific antibodies. J. Biol. Chem. **275**, 33836-33843.

26 Wang, X., Beugnet, A., Murakami, M., Yamanaka, S. and Proud, C.G. (2005) Distinct signaling events downstream of mTOR cooperate to mediate the effects of amino acids and insulin on initiation factor 4E-binding proteins. Mol. Cell. Biol. **25**, 2558-2578.

27 Lin, T.A., Kong. X., Haystead, T.A., Pause, A., Belsham, G., Sonenberg, N. and Lawrence, J.C. Jr (1994) PHAS-I as a link between mitogen-activated protein kinase and translation initiation. Science **266**, 653-656

28 Pause, A., Belsham, G.J., Gingras, A.C., Donze, O., Lin, T.A,. Lawrence, J.C. Jr, and Sonenberg, N. (1994) Insulin-dependent stimulation of protein synthesis by phosphorylation of a regulator of 5'-cap function. Nature **371**, 762-767

29 Karim, M.M., Hughes, J.M.X., Warwicker, J., Scheper, G.C., Proud, C.G. and McCarthy, J.E.G. (2001) A quantitative molecular model for modulation of mammalian translation by the eIF4E-binding protein 1. J. Biol. Chem. **276**, 20750-20757

30 Proud, C.G. (2007) Signalling to translation: how signal transduction pathways control the protein synthetic machinery. Biochem. J. **403**, 217-234

31 Gingras, A.C., Raught, B., Gygi, S.P., Niedzviewiecka, A., Miron, M., Burley, S.K., Polakiewicz, R.D., Wyslouch-Cieszynska, A., Aebersold, R., and Sonenberg, N. (2001) Hierarchical phosphorylation of the translation inhibitor 4E-BP1. Genes & Dev **15**, 2852-2864

32 Martin de la Vega, C., Burda, J., Nemethova, M., Quevedo, C., Alcazar, A., Martin, M.E., Danielisova, V., Fando, J.L. and Salinas, M. (2001) Possible mechanisms involved in the down-regulation of translation during transient global ischaemia in the rat brain. Biochem. J. **357**, 819-826

33 Aarts, M., Liu, Y., Liu, L., Besshoh, S., Arundine, M., Gurd, J.W., Wang, Y.T., Salter, M.W. and Tymianski, M. (2002) Treatment of ischemic brain damage by perturbating NMDA receptor- PSD-95 protein interactions. Science **298**, 846-850

34 Dawson, V.L., Dawson, T.M., Bartley, D.A., Uhl, G.R. and Snyder, S.H. (1993) Mechanisms of nitric oxide-mediated neurotoxicity in primary brain cultures. J. Neurosci. **13**, 2651-2661

35 Bonfoco, E., Leist, M., Zhivotovsky, B., Orrenius, S., Lipton, S.A., and Nicotera, P. (1996) Cytoskeletal breakdown and apoptosis elicited by NO donors in cerebellar granule cells require NMDA receptor activation. J. Neurochem. **67**, 2484-2493

36 Golde, S., Chandran, S., Brown, G.C. and Compston, A. (2002) Different pathways for iNOS-mediated toxicity in vitro dependent on neuronal maturation and NMDA receptor expression. J. Neurochem. **82**, 269–282.

37 Bal-Price, A. and Brown, G.C. (2001) Inflammatory neurodegeneration mediated by nitric oxide from activated glia-inhibiting neuronal respiration, causing glutamate release and excitotoxicity. J. Neurosci. **21**, 6480–6491

38 Pall, M.L. (2002) NMDA sensitization and stimulation by peroxinitrite, nitric oxide and organic solvents as the mechanism of chemical sensitivity in multiple chemical sensitivity. FASEB J. **16**, 1407-1417

39 Volbracht, C., Chua, B.T., Ng, C.P., Bahr, B.A., Hong, W. and Li, P. (2005) The critical role of calpain versus caspase activation in excitotoxic injury induced by nitric oxide. J. Neurochem. **93**, 1280-1292

40 Brorson, J.R., Schumacker, P.T., and Zhang, H. (1999) Nitric oxide acutely inhibits neuronal energy production. J. Neurosci. **19**, 147-156

41 Meli, E., Pangallo, M., Baronti, R., Chiarugi, A., Cozzi, A., Domenico E. Pellegrini-Giampietro, D.E., and Moroni F. (2003) Poly(ADP-ribose) polymerase as a key player in excitotoxicity and post-ischemic brain damage. Toxicol. Lett. **139**:153-162

42 Muñoz, F., Martín, M.E., Manso-Tomico, J., Berlanga, J., Salinas, M., and Fando, J. L. (2000) Ischemia-induced phosphorylation of initiation factor 2 in differentiated PC12 cells: role for initiation factor 2 phosphatase. J. Neurochem. **75,** 2335–2345

43 Moore, J.D., Rothwell, N.J. and Gibson, R.M. (2002) Involvement of caspases and calpains in cerebrocortical neuronal cell death is stimulus-dependent. Br. J. Pharmacol. **35**, 1069-1077

44 Sattler, R., Xiong, Z., Lu, W.Y., Hafner, M., MacDonald, J.F. and Tymianski, M. (1999) Specific coupling of NMDA receptor activation to nitric oxide neurotoxicity by PSD-95 protein. Science **284**, 1845-1848

45 Dawson, V., Kizushi, V.M., Huang, P.L., Snyder, S.H. and Dawson, T.M. (1996) Resistance to neurotoxicity in cortical cultures from neuronal nitric oxide synthase-deficient mice. J. Neurosci. **16**, 2479-2487

46 DeGracia, D.J. (2004) Acute and persistent protein synthesis inhibition following cerebral reperfusion. J. Neurosci. Res. **77**, 771-776

47 García, L., Burda, J., Hrehorovska, M., Burda, R., Martin, M.E. and Salinas, M. (2004) Ischaemic preconditioning in the rat brain: effect on the activity of several initiation factors, Akt and extracellular signal-regulated protein kinase phosphorylation, and GRP78 and GADD34 expression. J. Neurochem. **88**, 136-147

48 Planas, A.M., Soriano, M.A., Estrada, A., Sanz, O., Martin, F. and Ferrer, I. (1997) The heat shock stress response after brain lesions: induction of 72 kDa heat shock protein (cell types involved, axonal transport, transcriptional regulation) and protein synthesis inhibition. Progress Neurobiol. **51**, 607-636.

49 Piñeiro, D., González, V.M., Hernández-Jiménez, M., Salinas, M, and Martin, M.E. (2007) Translation regulation after taxol treatment in NIH3T3 cells involves the elongation factor (eEF)2. Exp. Cell Res. **313**, 3694-3706.

50 García-Bonilla, L., Burda, J., Piñeiro, D., Ayuso, I., Gómez-Calcerrada, M. and Salinas, M. (2006) Calpain-induced proteolysis after transient global cerebral ischemia and ischemic tolerance in a rat model. Neurochem. Res. **31**, 1433-1441.

Figure legends

Figure 1 Neuronal death induced by NMDA and NO

A. Neuron-enriched cortical cultures at 11-12 DIV were co-incubated with 2 mM L-NAME plus 100 µM NPLA (NOSI) and NMDA for 30 min. Medium was then removed and replaced with fresh medium supplemented with the same concentration of NOS inhibitors. Lactate dehydrogenase activity was determined 24 h later as indicated in Methods. Values in arbitrary units are mean ± SEM of 4-8 individual determinations. B. Mixed cultures were treated with NMDA and NOSI as indicated in A. At 24 h post-injury, cells were fixed and stained with PI as indicated in Methods. The number of PI-stained nuclei was counted under the fluorescence microscope (see Methods). Results are expressed as PI-positive neurons/mm^2. Values are mean ± SEM of 6 replicates per condition from two different experiments. C. Dose-response study (4-40 µM) for DEA/NO toxicity in mixed cultures. Lactate dehydrogenase activity was determined in culture media 24 h after a 30-min exposure to DEA/NO. Values are mean ± SEM of 7-8 replicates from two different experiments. Significance for all graphs:*P<0.05, ***P<0.001 vs. control cultures; $^{\$\$\$}$P<0.001 vs. NMDA-treated cultures. C=control, N=NMDA, NOSI=NOS inhibitors (NAME+NPLA). N+NOSI=NMDA+NOS inhibitors.

Figure 2 Long-lasting inhibition of protein synthesis induced by NMDA and NO in cortical cultures

A. Protein synthesis was assessed by incorporation of [^{3}H]leucine into proteins in mixed cultures as detailed in Methods. [^{3}H]leucine was added simultaneously with NMDA (0.5 h), 30 min (1 h) or 90 min (2 h) after a 30-min incubation with NMDA. NOS inhibitors were added immediately before NMDA and after NMDA removal. Results were calculated as dpm/mg prot/min and expressed as % control (n=4-16). B. Incorporation of [^{3}H]leucine into proteins in neuron cultures was performed as for mixed cultures and detailed in Methods. Data are mean ± SEM (n=4-15). C. Protein synthesis was assessed by incorporation of [^{3}H]leucine into proteins in neuron cultures as detailed in Methods. [^{3}H]leucine was added simultaneously with DEA/NO (0.5 h) or 90 min (2 h) after a 30-min incubation with DEA/NO 40 µM. Results were calculated as dpm/mg prot/min and expressed as % control. Data are mean ± SEM (n=9-17). Significance for all graphs: *P<0.05, **P<0.01, ***P<0.001 vs. control cultures; $^{\$\$\$}$P<0.001 vs. NMDA-treated cultures. C=control, N=NMDA, NOSI=NOS inhibitors (NAME+NPLA), N+NOSI=NMDA+NOS inhibitors. Bars in the graphs represent the incubation duration with NMDA or DEA/NO.

Figure 3 Effect of NMDA and NO on ATP content and phosphorylation status of eIF2α

A. Neuron-enriched cultures were incubated for 30 min with NMDA. Cells were scrapped either at the end of the 30-min incubation (0.5 h) or 90 min after medium change (2 h) and processed for ATP determination as detailed in Methods. Results were calculated as nmol/mg protein and expressed as % control. Data are mean ± SEM of 8-18 replicates. B. Neuron-enriched cultures were treated for 30 min with DEA/NO. ATP content was determined at 0.5 h or 2 h after DEA/NO as in A. Data are mean ± SEM of 10-20 replicates from three different experiments. C. Neuron-enriched cultures were co-incubated for 30 min with NMDA and NOS inhibitors. Cells were scraped 90 min after medium change and processed for ATP determination as detailed in A. Data are mean ± SEM of 9 replicates for each condition from two different experiments. Neuron-enriched cultures were treated with NMDA or NMDA+NOSI (D) or with DEA/NO (E) for 30 min. Ninety minutes later, cells were collected, proteins were separated on 12% SDS-PAGE and processed for Western blot as indicated in Methods. Membranes were incubated first with an eIF2α-P antibody and then reprobed with the antibody recognizing eIF2α independently of its phosphorylation state.

Bottom panels are quantitative analysis of the blots. Band density was measured, the eIF2α-P/eIF2α total ratio was calculated for each sample and results are expressed as % control. Data are mean ± SEM of 11-13 replicates in D and 9-12 replicates in E. Significance for all graphs: *P<0.05, ***P<0.001 vs. control cultures; $^{\$\$}$P<0.01 vs. NMDA-treated cultures. Unpaired t-test was performed for statistical analysis in E. F. Neurons were treated with thapsigargin for 30 min and phosphorylation of eIF2α was examined by Western blot as described in D. C=control, N=NMDA, N+NOSI=NMDA+NOS inhibitors (NAME+NPLA), Thap=thapsigargin.

Figure 4 α-spectrin and eIF4G cleavage after NMDA and NO

A. NMDA leads to the proteolysis of α-spectrin and eIF4G. Neuron cultures were exposed to NMDA or NMDA+NOS inhibitors for 30 min as in Fig 3D. Proteins were separated on 7% SDS-PAGE and processed for eIF4G immunoblotting. Membranes were then reprobed with an antibody recognizing α-spectrin. NMDA treatment induced a loss of eIF4G (bottom blot) and of full-length α-spectrin and the generation of the 150 kDa spectrin fragment but not of the 120 kDa product (lowest band, top blot). NOS inhibitors impeded spectrin and eIF4G proteolysis. B. Neuron cultures were exposed for 30 min to DEA/NO as in Figure 3E. Proteins were processed for eIF4G and α-spectrin Western blot as in A. DEA/NO triggered calpain-mediated breakdown of spectrin (top blot) and eIF4G (bottom blot). Blots are representative of two different experiments. C. Quantitative analysis of cleaved spectrin (top graph) and eIF4G (bottom graph). Cells were treated as in A. Results were calculated as arbitrary units and expressed as % control. Data are mean ± SEM of 4-6 replicates for spectrin and 8-13 for eIF4G. D. Quantitative analysis of cleaved eIF4G after DEA/NO treatment. Cells were treated as in B. Data are mean ± SEM of 7 replicates. Significance for all graphs:*P<0.05, **P<0.01 vs. control cultures and $^{\$}$P<0.05, $^{\$\$\$}$P<0.001 vs. NMDA-treated cultures. C=control, N=NMDA, N+NOSI=NMDA+NOS inhibitors (NAME+NPLA).

Figure 5 Effect of calpain inhitors on α-spectrin and eIF4G cleavage

A. Neuron-enriched cultures were pre-treated for 1 h with 30 μM calpeptin and exposed to NMDA for 30 min. B. Neuron-enriched cultures were pre-treated for 1 h with 30 μM MDL28170 and then exposed to DEA/NO. Sister cultures were treated with vehicle. Ninety minutes after medium change, cells were collected and processed for eIF4G and α-spectrin Western blot as in Figure 4. The calpain inhibitors completely blocked spectrin and eIF4G proteolysis. C. Quantitative analysis of cleaved spectrin (top graph) and eIF4G (bottom graph). Cells were treated as in A. Data are mean ± SEM of 5 replicates for spectrin and 9-10 for eIF4G. D. Quantitative analysis of cleaved spectrin (top graph) and eIF4G (bottom graph). Cells were treated as in B. Data are mean ± SEM of 9-10 replicates. Significance for all graphs: *P<0.05, ***P<0.001 vs. control cultures and $^{\$}$P<0.05, $^{\$\$}$P<0.01 or $^{\$\$\$}$P<0.001 vs. NMDA- or DEA/NO-treated cultures. C=control, N=NMDA, N+NOSI=NMDA+NOS inhibitors (NAME+NPLA), D=DEA/NO, Cp= calpeptin and M=MDL28170.

Figure 6 Phosphorylation status of 4E-BP1 and eIF4E/eIF4G complexes formation after NMDA and NO. Effect of calpain inhibitors on 4E-BP1 dephosphorylation and protein synthesis inhibition induced by NMDA or DEA/NO.

A. Neuron-enriched cultures were treated with NMDA or NMDA+NOS inhibtors for 30 min and 90 min after medium change, cells were collected and processed for eIF4E Western blot. B. Cultures were pretreated for 1 h with 30 μM calpeptin or MDL28170. Then NMDA or DEA/NO were added to the culture medium. Thirty minutes later, medium was changed and replaced with fresh medium containing the same concentration of calpain inhibitors. Sister cultures were treated with NMDA or NMDA+NOS inhibitors. Ninety minutes after medium

change, cells were collected and processed for 4E-BP1 Western blot. C. Cultures were treated with NMDA or NMDA+NOS inhibitors or DEA/NO. Ninety minutes after NMDA or DEA/NO exposure, cells were processed for the purification of eIF4E by m^7GTP-sepharose affinity chromatography. Proteins were then eluted in SDS loading buffer and subjected to 7.5%-17% SDS-PAGE followed by Western blot for eIF4G, eIF4E and 4E-BP1, as described in Methods. D. Neuron-enriched cultures were pre-treated for 1 h with 30 μM calpeptin or MDL28170. NMDA or DEA/NO were then added to the culture medium. Thirty minutes later, the medium was changed and replaced with fresh medium containing the same concentration of calpain inhibitors. Ninety minutes after medium change, cells were incubated for 30 min with [^{3}H]leucine and then processed for the determination of leucine incorporated into proteins, as detailed in Methods. Results calculated in dpm/mg prot/min are presented as mean ± SEM of 4-9 replicates from two different cultures. None of the calpain inhibitors impeded NMDA- or DEA/NO-induced translation inhibition. E. Cultures were treated as in D. LDH activity was determined 24 h later. Results proceeding from two different experiments are expressed in arbitrary units. Data are mean ± SEM of 7-16 replicates. None of the inhibitors enabled rescue from neuronal death induced by NMDA or DEA/NO. Significance for both graphs: ***P<0.001 vs. control cultures; $^{\$}$P<0.05 vs. NMDA-treated cultures. C=control, N=NMDA, N+NOSI=NMDA+NOS inhibitors (NAME+NPLA), D=DEA/NO, Cp=calpeptin, M=MDL28170.

Figure 7 Effect of rapamycin on phosphorylation status of 4E-BP1, eIF4E/eIF4G complexes formation and protein synthesis

Neuron-enriched cultures were treated for 3 h with rapamycin (1 or 2 μM) or vehicle and were then processed for eIF4G or 4E-BP1 Western blot (A) or for eIF4E purification and subsequent determination of the eIF4E/eIF4G and eIF4E/4E-BP1 complexes (B). C. Protein synthesis was assessed by incorporation of [^{3}H]leucine into proteins in neuron cultures 3 h after addition of rapamycin (1 or 2 μM) or vehicle as detailed in Methods. Results were calculated as dpm/mg prot/min and expressed as % control (n=5-11). Significance: **P<0.01 and **P<0.001 vs. control cultures. Rap=rapamycin.

Figure 8 NMDA targets responsible for delayed translation repression

Following the stimulation of NMDA receptors, NO is produced and induces the hypophosphorylation of 4E-BP1 and the subsequent binding to eIF4E, thus reducing its availability to interact with eIF4G. Increased intracellular calcium activates calpain that cleaves eIF4G into fragments unable to bind eIF4E. Lower amounts of full-length eIF4G together with the sequestration of eIF4E result in the formation of fewer eIF4E/eIF4G complexes and translation inhibition. Alterations of additional translation factors by regulation of phosphorylation status and/or degradation most likely contribute to achieve the full inhibition of translation.

Table 1 Phosphorylation status of 4E-BP1 after NMDA and NO. Effect of calpain or NOS inhibitors

	Isoforms		
	Gamma	Beta	Alpha
Control	34.9±5.6	42.9±4.7	22.2±4.7
NMDA	28.3±5.2	39.7±4.9	32.0±5.4**
NMDA+NOSI	39.4±5.6$^{\$\$}$	42.3±4.1	18.3±4.4$^{\$\$\$}$
DEA/NO	24.4±6.2**	38.8±2.7	36.8±3.8***
Control	39.1 ±1.7	39.9±1.6	20.4±0.8
NMDA	30.0±2.9	41.0±1.2	29.0±2.0*
NMDA+Calpeptin	23.2±2.3***	40.4±0.9	36.4±2.3$^{***,\$}$
Control	33.2±1.4	43.8±1.3	23.0±1.7
DEA/NO	23.3±1.7*	40.9±0.6	35.9±1.7**
DEA/NO+MDL28170	22.6±3.6*	39.9±0.7*	37.5±3.6**

Neuron-enriched cultures were treated with NMDA, NMDA+NOS inhibitors or DEA/NO for 30 min. Calpain inhibitors were added as described in Figure 5. Ninety minutes after NMDA or DEA/NO removal, cells were collected and processed for 4E-BP1 Western blot. For each sample, the proportion of each phosphorylated form of 4E-BP1 (α, β and γ) was calculated as the percentage of each band over the total as explained in Methods. Data are mean ± SEM of 5-10 replicates. Significance: *P<0.05, **P<0.01, ***P<0.001 vs. control cultures and $^{\$}$P<0.05, $^{\$\$}$P<0.01 or $^{\$\$\$}$P<0.001 vs. NMDA-treated cultures. NOSI=NOS inhibitors.

Biochemical Journal Immediate Publication. Published on 16 Jan 2008 as manuscript BJ20071060

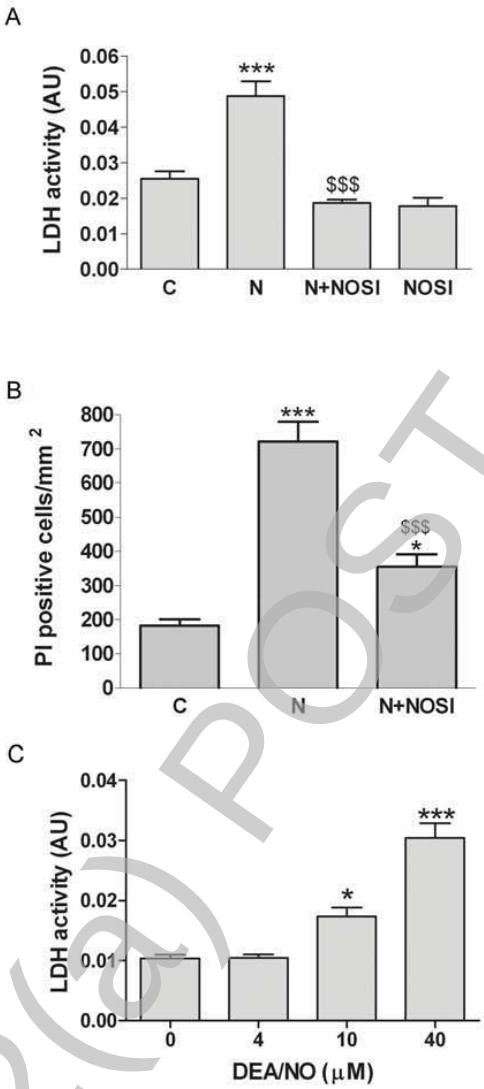

Figure 1.

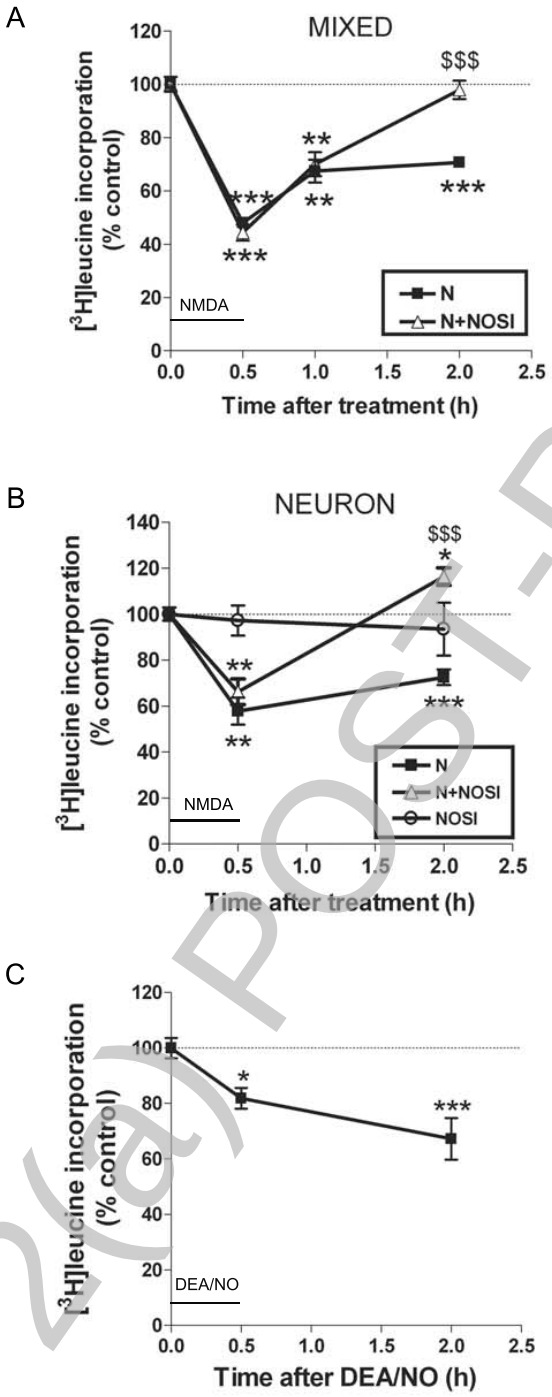

Figure 2

Biochemical Journal Immediate Publication. Published on 16 Jan 2008 as manuscript BJ20071060

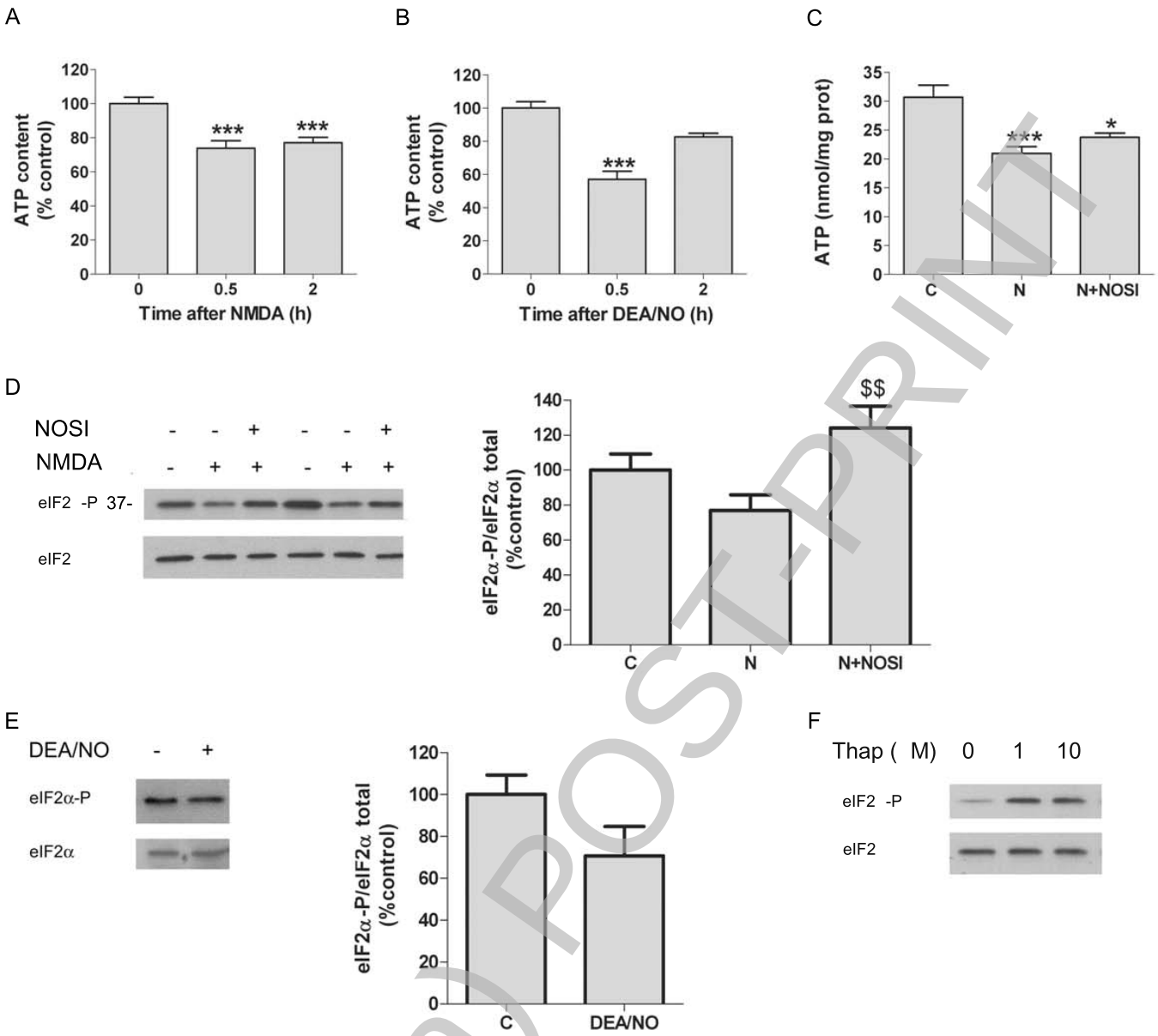

Figure 3

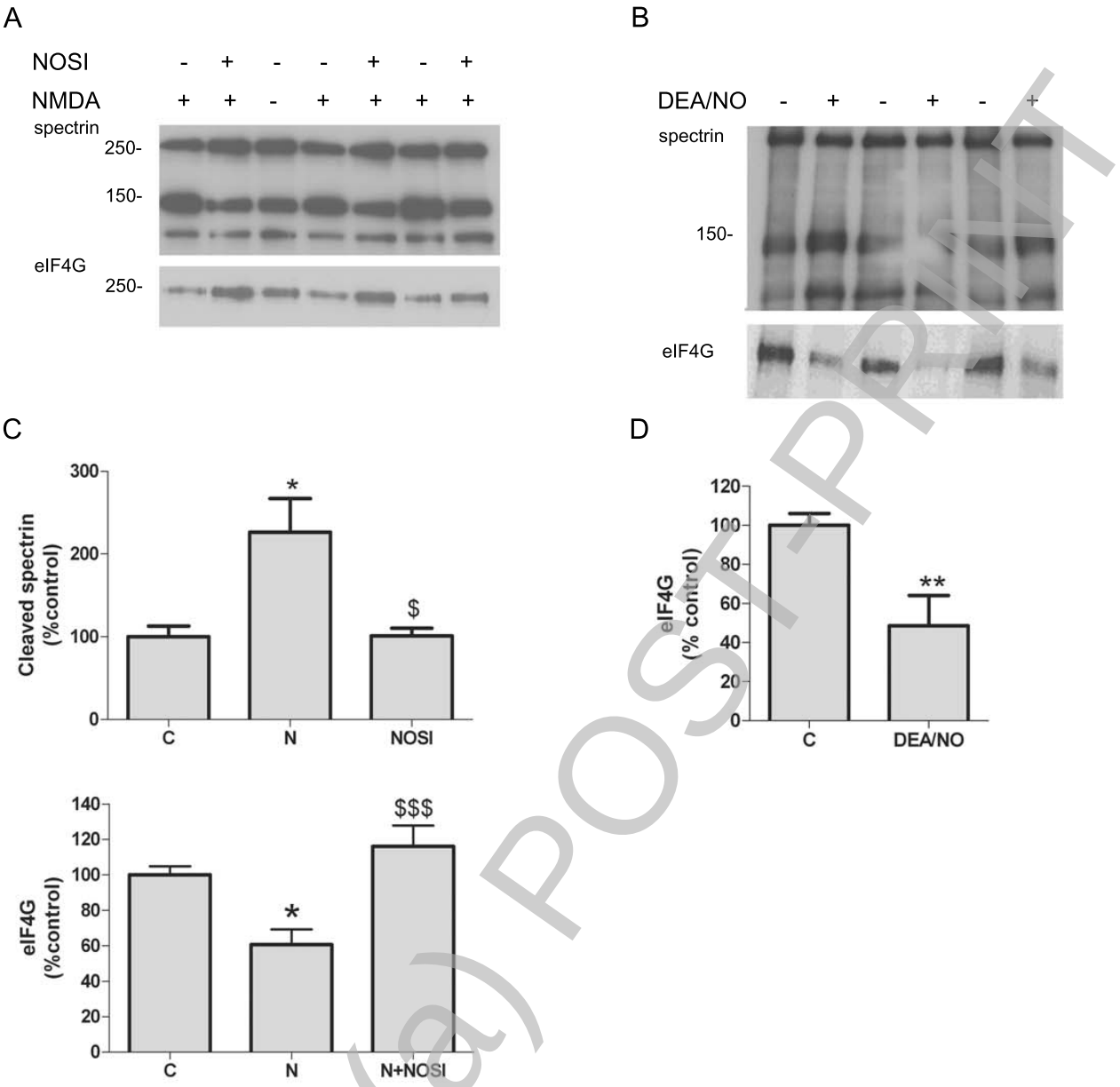

Figure 4

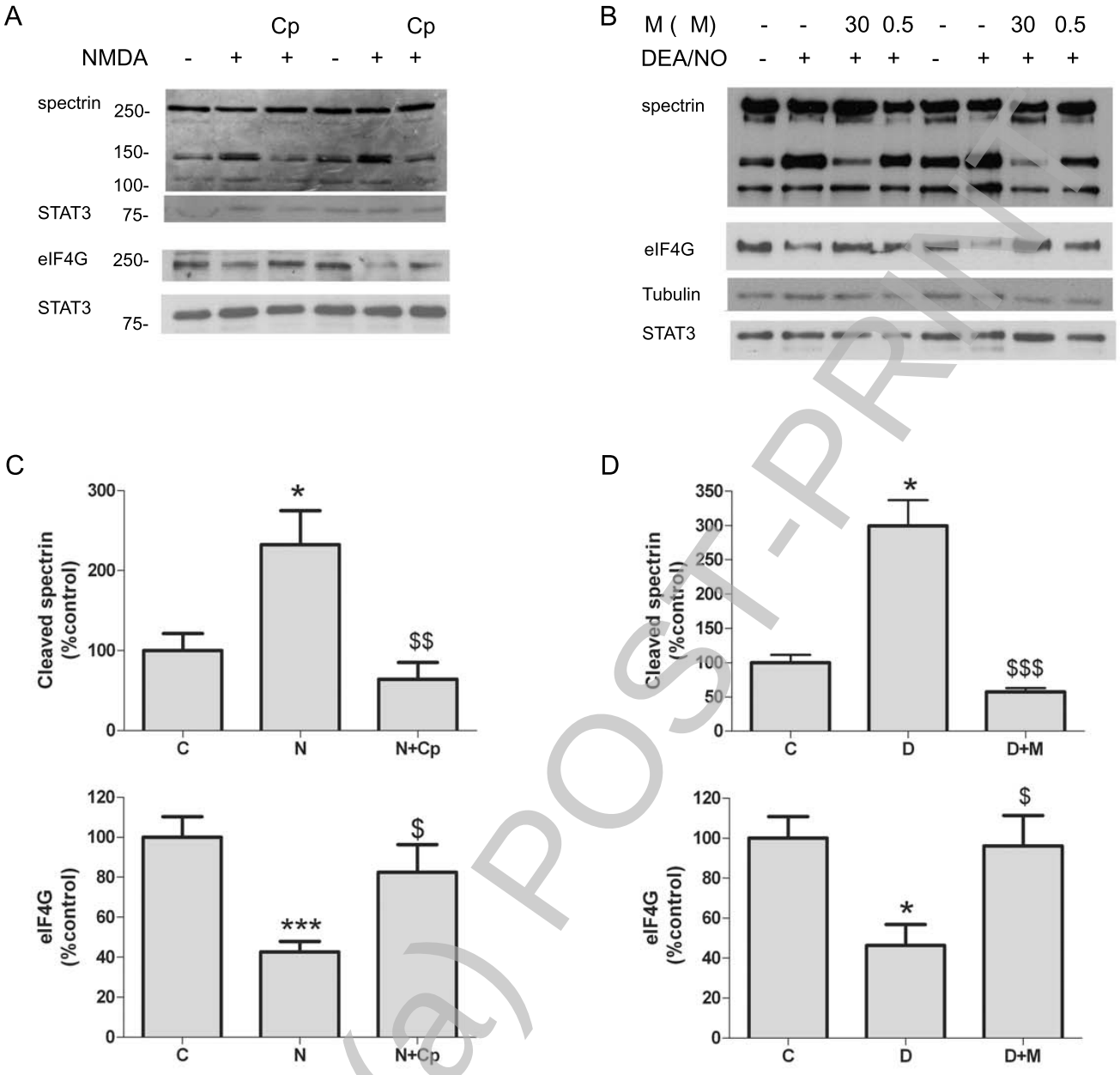

Figure 5

Biochemical Journal Immediate Publication. Published on 16 Jan 2008 as manuscript BJ20071060

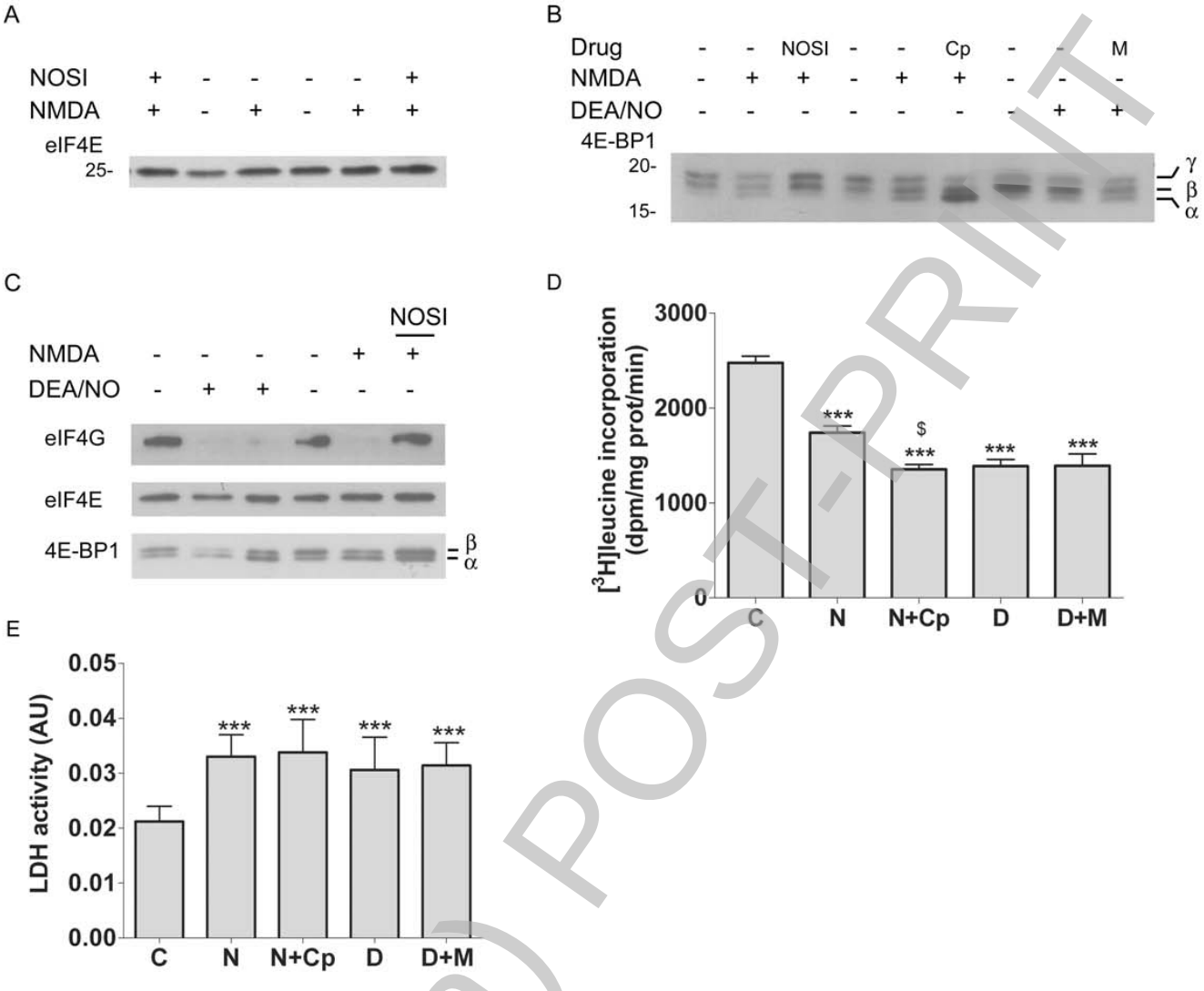

Figure 6

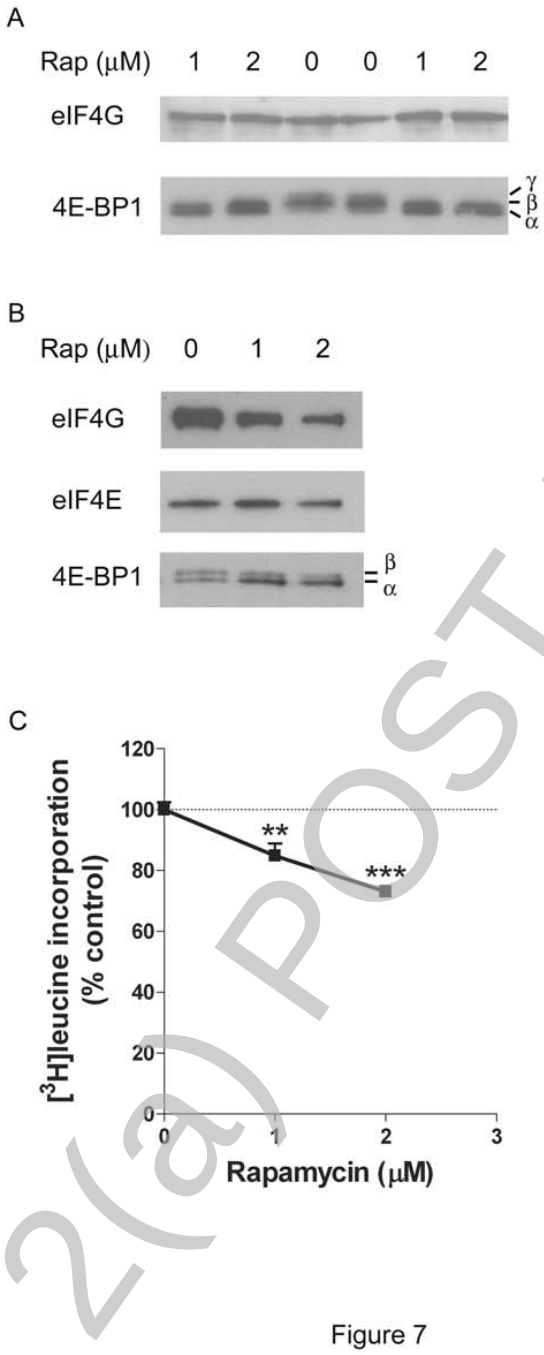

Figure 7

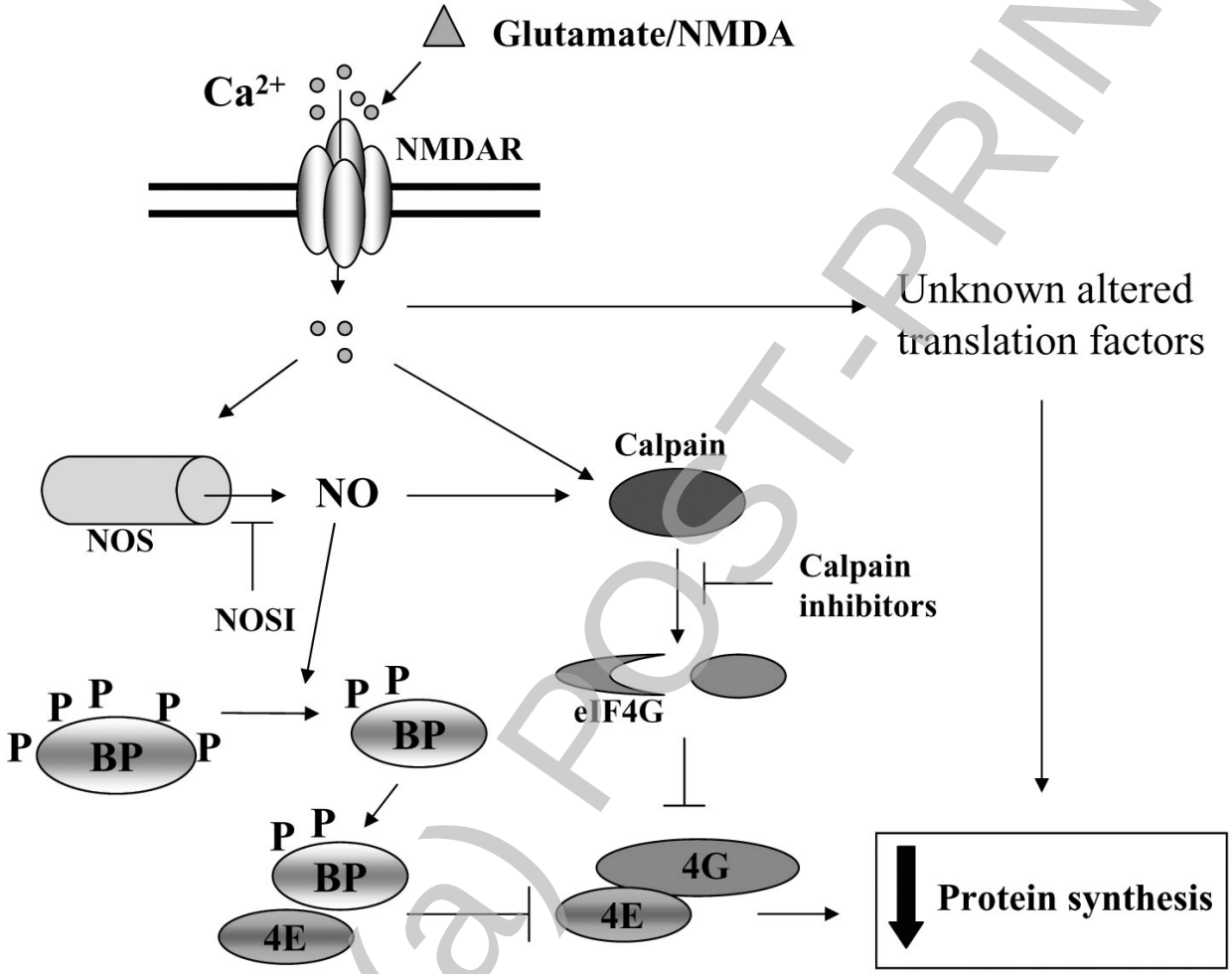

Figure 8